IDO-16693

QUARTERLY TECHNICAL REPORT
SPERT PROJECT

January, February, March, 1961

F. Schroeder, Ed.

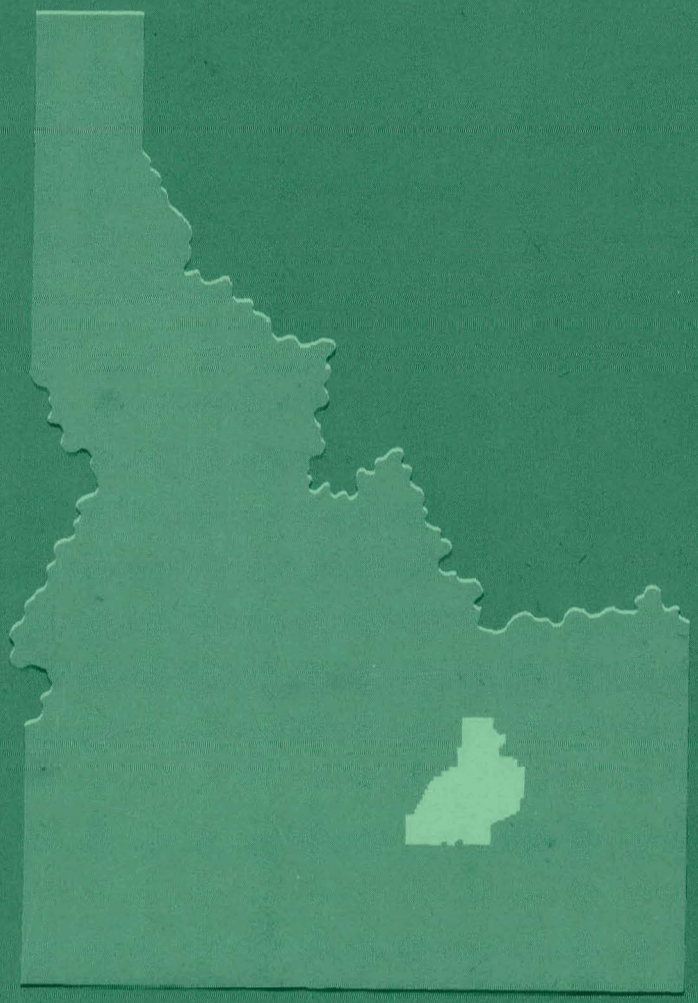

PHILLIPS PETROLEUM COMPANY

ATOMIC ENERGY DIVISION

NATIONAL REACTOR TESTING STATION

US ATOMIC ENERGY COMMISSION

DISCLAIMER

PRICE $ .75

Available from the
Office of Technical Services
U. S. Department of Commerce
Washington 25, D. C.

Printed in USA

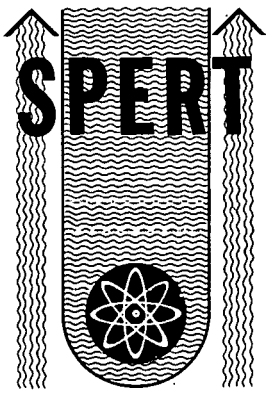

SPECIAL POWER EXCURSION REACTOR TESTS

IDO-16693
AEC Research and Development Report
Reactor Technology
TID-4500 (16th Ed.)
Issued: June 30, 1961

QUARTERLY TECHNICAL REPORT
SPERT PROJECT
JANUARY, FEBRUARY, MARCH, 1961

J. R. Huffman
Assistant Manager, Technical

W. E. Nyer
Manager, Reactor Projects Branch

F. Schroeder
Manager, Spert Project

PHILLIPS
PETROLEUM
COMPANY

Atomic Energy Division
Contract AT(10-1)-205
Idaho Operations Office
U. S. ATOMIC ENERGY COMMISSION

Previous Quarterly Reports

Spert Project

1957

Quarter	Report No.
3	IDO-16416
4	IDO-16437

1958

1	IDO-16452
2	IDO-16489
3	IDO-16512
4	IDO-16537

1959

1	IDO-16539
2	IDO-16584
3	IDO-16606
4	IDO-16616

1960

1	IDO-16617
2	IDO-16640
3	IDO-16677
4	IDO-16687

TABLE OF CONTENTS

LIST OF FIGURES

LIST OF TABLES

I. SUMMARY

SPERT I - A core comprised of 4%-enriched UO_2 powder compressed into 6 ft long, 0.5 in. diameter fuel pins has been installed in the Spert I reactor. A program of reactor kinetics investigations is to be performed for this core. Because of the long thermal time constants for these fuel pins, the most significant reactivity compensating mechanism is expected to be due to the Doppler broadening of the U^{238} neutron absorption resonances as the fuel temperature increases. This nuclear contribution to the negative temperature coefficient of the reactor is prompt in its effect in contrast to the delayed moderator-void reactivity effects associated with the transfer of heat from fuel element to moderator which were predominant in previously tested plate-type, highly enriched cores. The investigation of the effectiveness of the Doppler broadening as a quenching mechanism is a primary objective of the forthcoming Spert I test program.

A core loading comprised of 592 fuel pins was found to have an available excess reactivity of about $3, and will be used for the kinetic tests. Integral and differential rod worth data have been obtained for this core and the reactivity worth of individual fuel pins has been determined as a function of position in the core.

Examination of the results of the large-amplitude, low-power oscillator tests previously performed in Spert I has continued in an attempt to explain a discrepancy between the neutron-amplitude results and the "describing-function" predictions at frequencies below 0.5 cps. The compensated ion chamber which had been used as a neutron detector for the oscillator tests has been checked by the performance of oscillator tests in the Treat reactor. The data obtained were in good agreement with those obtained with a Treat-owned chamber and the results from both chambers were in satisfactory agreement with predicted values for the Treat reactor. It is concluded that, except for the possible effect of chamber microphonics which has not yet been checked, the anomaly in the Spert I pile oscillator test data is not attributable to faulty operation of the neutron detector used.

SPERT II - The first self-limiting power-excursion test with a D_2O-moderated reactor was performed in Spert II on February 21, 1961. The test was the first of a series designed to investigate the dynamic response of a D_2O-moderated core in which 3 in. x 3 in. highly enriched, plate-type, aluminum-clad fuel assemblies are spaced on 6-in. centers. The initial test series consisted of power excursions initiated by step-wise reactivity insertions in the range from approximately 40¢ to $3, which resulted in a range of initial asymptotic periods from 10 sec to 50 msec. The tests were performed at ambient temperature, atmospheric pressure, and with no forced coolant flow. Preliminary examination of the data indicates that the behavior is in essential agreement with predictions for the long-lifetime system. Both the power and fuel plate surface temperature data suggest that steam formation is an important quenching mechanism for tests with initial periods as long as 150 msec and that, in the post-burst region, bulk boiling is taking place within the fuel assemblies. The importance of boiling as a reactivity compensating mechanism at relatively long periods is a reasonable consequence of the large reactivity compensations required because of the long prompt neutron lifetime of this core. For

tests with periods of 70 to 50 msec, transient pressure differentials in the core have been sufficient to cause deformation of fuel plates. The statistical nature of the bulk-boiling process, which produces considerable variations in local heat transfer rates, has resulted in uncertainty in the location and magnitude of the maximum fuel plate surface temperature.

SPERT III - Previously reported data have indicated that, by elevation of the primary system pressure in the Spert III reactor, boiling can be suppressed as a reactivity compensating mechanism for power excursions with periods as short as 10 msec. The reactor power bursts for these tests are only slightly different from those for unpressurized tests, and it has been thought that the reactivity compensation due to fuel plate expansion and moderator heating by conduction must be sufficient to quench the power burst. Calculations have now been performed to evaluate the total reactivity contribution from these mechanisms and the results have been compared with the reactivity compensation at the time of peak power obtained by analysis of the power history. The comparison indicates that, while the variation in the calculated compensated reactivity with reciprocal period is essentially the same as for the experimental data, the magnitude of the calculated values is only about half that of the experimental. Even if $\pm 20\%$ deviation in each of the input data is assumed, the resultant maximum probable deviation in the calculated results is $\pm 50\%$. The failure of this method of analysis to adequately predict the observed reactivity compensation suggests the need for further consideration of other mechanisms and of possible radiation effects on heat transfer rates.

Tests have been performed to investigate the response of the Spert III reactor to reactivity additions which are linear functions of time. These ramp-rate tests were initiated from delayed critical at room temperature for various initial power levels from 0.1 w to 100 kw, system pressures from 0 to 2500 psig, and coolant flow rates from 0 to 20,000 gpm. Reactivity addition rates of 53, 35 and 18¢/sec were employed. As had previously been found for Spert I, the power-burst behavior is quite sensitive to reactivity addition rate, and relatively insensitive to initial power level in the range investigated. For practical purposes, the power excursions resulting from ramp additions and step-wise additions of reactivity are essentially equivalent when compared on the basis of effective period. In addition, it has been demonstrated that the effects of changes in system pressure and coolant flow rate on the power excursion behavior are essentially independent of the mode of reactivity insertion.

ENGINEERING - Because of a recent fatigue failure of a primary system thermowell in Spert III, the existing thermowell installations have been examined with respect to their vibration frequency spectra for various primary coolant flow rates. Twelve of the wells were found to have natural resonant frequencies in close proximity to the frequency of the primary pump impellers. These wells have been removed and replaced with shorter thermowells which have been shown to be relatively unaffected by either vortex excitation or pump impeller frequencies.

A hydraulic fatigue test has been conducted on an 18-plate, type "D" fuel assembly. At the completion of the 220 hour test with a flow of 41 ft/sec in the fuel assembly water channels, no apparent physical damage had occurred to the plates.

II. SPERT I

A. Spert I Oxide-Core Experimental Program

1. Introduction

The increasing importance of the heterogeneous, water-moderated, slightly enriched oxide core as a power reactor concept has emphasized the need for a program of kinetic tests on this type of core as a part of the overall reactor safety program being carried out at Spert. To date, the experimental effort at Spert has been directed toward investigations of the highly enriched, plate-type, water-moderated reactor, for which class of reactor considerable data have been amassed in regard to dynamic behavior and shutdown properties under short-period transient conditions. The information gained on several cores, encompassing wide variations in size, fuel loading, metal-to-water ratio, prompt neutron lifetime, void coefficient and other core properties, has indicated that the observed reactor response during self-limiting power excursion tests is primarily determined for these undermoderated reactors by the inherent decrease in reactivity afforded by loss of moderator. For plate-type reactors, where heat transfer from fuel plates to the water moderator takes place in times short compared with the reactor period, loss of moderator from the core occurs as a result of fuel plate expansion, water heating, formation of steam, and generation of radiolytic gas. With the possible exception of the last, these short-period quenching mechanisms will be relatively suppressed in a heterogeneous reactor comprised of low-enrichment UO_2 fuel rods in which the thermal time constants are long as a result of the low heat conductivity of the oxide fuel and the low surface-to-mass ratio of the cylindrical fuel elements. The low heat transfer properties of the oxide fuel rods will, during the course of a power excursion, give rise to large temperature gradients and cladding stresses in the fuel rods, and lead to the increased possibility of fuel element failure. In such a reactor, significant quenching is to be expected from the Doppler broadening of the U^{238} neutron absorption resonances as the fuel temperature increases. This nuclear contribution to the negative temperature coefficient of the reactor is prompt in its effect, in contrast with the delayed moderator-void reactivity effect associated with the transfer of heat from fuel element to moderator. Of basic importance, then, is the question of the effectiveness with which the Doppler shutdown mechanism, as determined by its magnitude and prompt character, acts to limit power excursions in a slightly enriched oxide reactor. The investigation of this effectiveness is a primary objective of the Spert I oxide-core experimental program.

2. Description of Core

The NS Savannah-type fuel pin[1] used in these experiments consists of welded-seam, stainless steel tube (6 ft long, 0.5 in. OD, with a 0.028 in. wall thickness) containing 1600 g of 4%-enriched UO_2

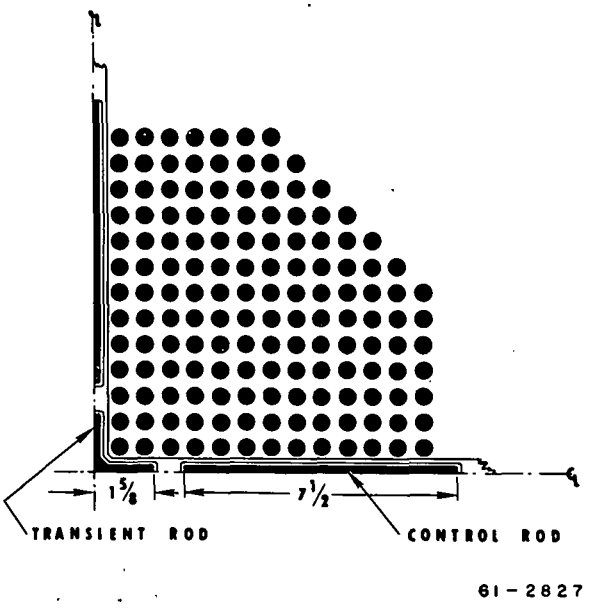

Fig. 1 - Quarter-Section of Spert I Oxide-Core Containing 592 Fuel Pins

powder compressed to an effective density of 9.45 g/cm^3, which is 87% of the theoretical density of UO_2.

The experimental core assembled in the Spert I, 4-ft-diameter, open tank is comprised of 592 fuel pins, with a center-to-center, rectangular fuel pin spacing of 0.663 in. A quarter-section through the core is shown in Fig. 1. The octagonal core section is divided into four quadrants by a 3/4-in.-thick aluminum rod-guide cross, which houses the four control rod blades and the cruciform transient rod. The poison sections of the control rod blades (56 in. x 7-1/4 in. x 3/8 in.) and of the transient rod (26-5/8 in. x 2-3/4 in. x 3/8 in.) are constructed of binal, an aluminum-boron alloy (7 wt% boron). The follower-sections of the control rods and transient rod are constructed of aluminum. The Spert I rod drive system restricts the vertical movement of the control rods to a travel of 21 in. In an effort to maximize rod worth, the control rods have been positioned axially so that the bottom tips of the poison sections move from the "inserted" (0 in.) rod position, which is 15.5 in. above the bottom of the active core region, to the "withdrawn" (21 in.) rod position at 36.5 in. above the bottom of the active core. The transient rod poison can be raised 21 in. into the bottom section of the core and rapidly ejected for the performance of excursion experiments.

3. Static Reactor Measurements

a. Fuel Loading. An initial critical loading was obtained with 503 fuel pins arranged in cylindrical geometry, for which an excess reactivity of 17¢ was measured when the control rods were raised to their outermost rod travel position of 21 in. (i.e., 36.5 in. above the bottom of the active core region). From a measure of the reactivity worth per fuel pin for a fuel pin at the perimeter of the core, the minimum critical core loading for this core was estimated to be 500 fuel pins. The loading of additional fuel to the core was continued until for a loading of 592 fuel pins an excess reactivity was obtained, which was somewhat greater than $3. For the 592 fuel pin core, the critical control rod position at ambient temperature (~ 15°C) was 7.9 in. The curve of critical rod position as a function of the number of fuel pins in the core is shown in Fig. 2. The reactivity results quoted above were obtained with the transient rod poison section out of the core.

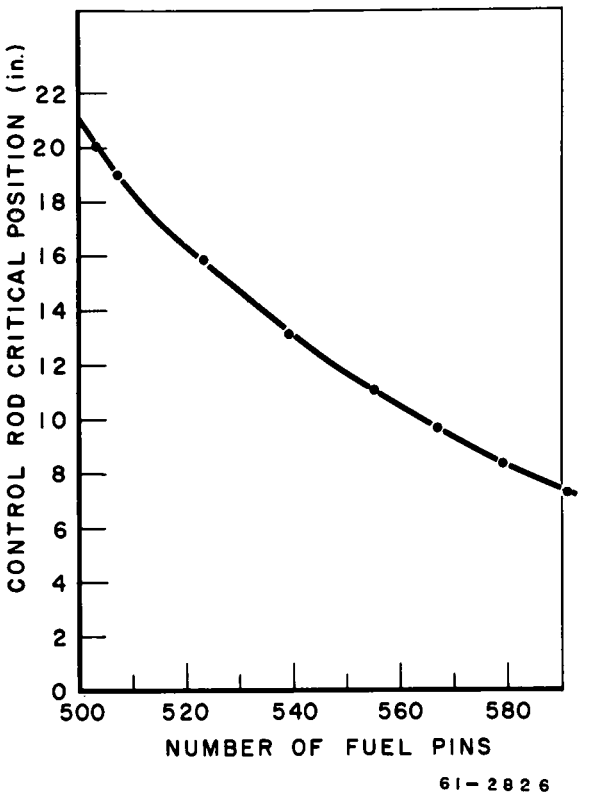

Fig. 2 - Control Rod Critical Position as a Function of Number of Fuel Pins for Spert I Oxide-Core

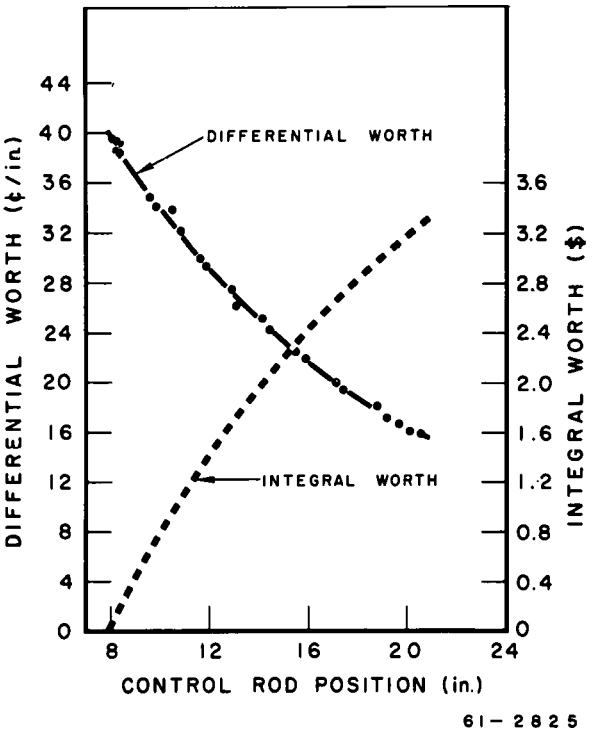

Fig. 3 - Differential and Integral Rod Worths for Spert I Oxide-Core

b. Rod Calibration. For the 592 fuel pin loading, reactivity calibration of the control rods was obtained over the range of rod travel of from 8 to 21 in., using a boron solution as a reactivity shim. The calibration curves of differential and integrated control rod worths are shown in Fig. 3. From these curves, the excess reactivity for the control rods at 21 in. is estimated to be $3.3. (An additional control rod calibration obtained during the fuel loading experiment yielded the same results, within experimental error, as those obtained for the 592 fuel pin core.) For the transient rod, intercalibration of the transient rod with the control rods indicated a total reactivity worth of nearly $3, which is estimated to be sufficient for carrying out step-transient experiments for reactor periods extending down to 5 msec.

c. Reactivity Worth Per Fuel Pin. The reactivity worth per fuel pin as a function of the radial position of the fuel pin was determined by measuring the change in critical position of the calibrated control rods with a given fuel pin in the core and with the pin removed from the core. The results obtained at different pin locations are listed in Table 1. Throughout most of the core, a negative reactivity effect is obtained upon insertion of a fuel pin. This is indicative of the degree of undermoderation that exists for this core.

TABLE 1

FUEL PIN REACTIVITY WORTH

Fuel Pin Lattice Position*	Reactivity Change When Fuel Pin is Inserted (cents)
(2,2)	-5.3
(4,4)	-5.5
(7,7)	-3.2
(10,10)	+2.8
(4,1)	-1.6
(7,1)	-1.2
(10,1)	-0.2

*Fuel pin position in any quadrant is given by the (x,y) coordinates of the pin, with the center of the core taken as the origin.

B. Analysis of Pile Oscillator Results

In a previous report[2], a discussion was presented of results obtained in pile oscillator tests carried out at low power in the Spert I P-18/19 reactor with large input reactivity amplitudes (up to about $0.15), the objective of these tests being to check a formulation by Akcasu[3] of the reactor "Describing Function" or amplitude-dependent transfer function. Satisfactory agreement with the theoretical predictions was obtained for the phase shift of the fundamental component of the neutron signal with respect to the input reactivity. The fundamental fractional neutron amplitude obtained experimentally, however, was increasingly too large, relative to the theoretical value, as the frequency was reduced below about 0.5 cps.

Several studies have been carried out in an attempt to explain this systematic discrepancy between theory and experiment. Among these studies was a thorough check of the compensated ion chamber, designed by Argonne National Laboratory, which had been used as neutron detector in the Spert pile oscillator tests. In addition to static calibration of the chamber at the MTR (which gave satisfactory results), the chamber

was installed in the Treat reactor, in conjunction with Treat pile oscillator studies, to compare its performance with that of an uncompensated ion chamber of similar design which had previously given good results.* The following is a brief summary of these tests in the Treat reactor.

A shadow-type, cadmium-aluminum, rotary reactivity oscillator was installed in the center of the Treat reactor. In this location, the reactivity amplitude was about \$0.064, and the reactivity wave shape contained about a 20% second-harmonic component. The Spert and Treat chambers were installed in symmetrical positions within the core, about 20 inches away from the oscillator and about 10 inches from the edge of the core. Oscillator tests were carried out at frequencies from 0.05 to 10.6 cps, using a nulling-type wave analyzer[4], and from 0.008 to 0.55 cps with direct recording of the neutron signals and subsequent Fourier analysis. The reactor power varied from about 70 to 150 w for the tests.

Within an estimated experimental error (90% confidence limits) of less than $\pm$1 degree in phase and about $\pm$2% in fractional neutron amplitude, no significant difference was found between the results from the two chambers. Furthermore, the results from both chambers were in satisfactory agreement with predicted values based on Akcasu's formulation, using the thermal-fission delayed-neutron data of Keepin and Wimett[5] and a value for the reduced prompt neutron lifetime of $(\ell/\beta)_{eff} = 0.125$ sec, based on the results of previous measurements at Treat[4]. A comparison with similarly calculated values based on the fast-fission delayed-neutron data of Keepin and Wimett was somewhat less satisfactory, the experimental amplitude results being in this case a few percent smaller at the lower frequencies compared to the theoretical values. Changing the delayed-neutron parameters in this way had only negligible effect on the calculated phase results.

It is concluded that (except for the possible effect of chamber microphonics, which was not tested in Treat Studies), the amplitude anomaly in the Spert pile oscillator test data is not due to faulty operation of the neutron-detecting ion chamber used.

---

*Performance of these tests was made possible by the cooperation and assistance of F. Thalgott and J. Boland of the Idaho Division of Argonne National Laboratory.

III. SPERT II

A. Initial Series of Power-Excursion Tests

The first self-limiting power-excursion test with a D_2O-moderated reactor was performed in Spert II on February 21, 1961. The test was the first of a series designed to investigate the dynamic response of the reactor with the core configuration shown in Fig. 4. This configuration of highly enriched, aluminum-clad fuel assemblies is designated as the BD-22/24 expanded core and has been previously described[6,7]. The initial test series consisted of self-limiting power excursions initiated by step-wise reactivity insertions from an initial power level of about 5 w. The tests were performed for an initial water temperature of about 20°C at atmospheric pressure and with no forced coolant flow. The range of initial asymptotic periods extended from 10 sec to 50 msec, corresponding to reactivity injections of approximately 40¢ to $3. The data from this series of tests provide a base point for investigation of the effect of the various system parameters on the kinetic behavior of the system, and also provide a basis for comparison of the behavior of this D_2O-moderated core with that of several H_2O-moderated cores previously tested at Spert.

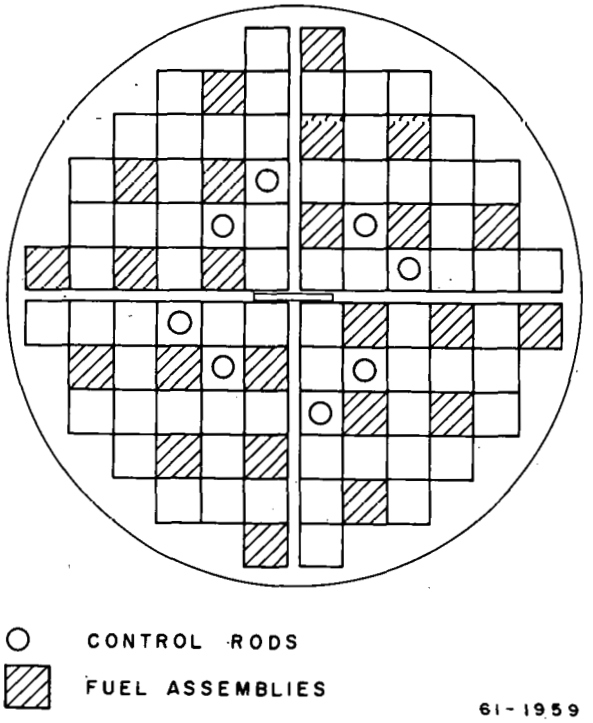

Fig. 4 - Spert II D_2O-Core Configuration

The preliminary Spert II data for maximum power as a function of reciprocal period are compared with those from a light-water core (Spert I, B-12/64) in Fig. 5. The B-12/64 core produced the largest peak powers for a given period of any of the previously tested Spert I cores[8].

Preliminary examination of the data from the fiducial test series for the D_2O-moderated system indicates that the general features of the behavior are those which would be expected for the long-lifetime system. Fig. 6 shows the power and the fuel plate surface temperature at a point near the center of the core as functions of time for a 150 msec-period test. The shape of the initial power burst is similar

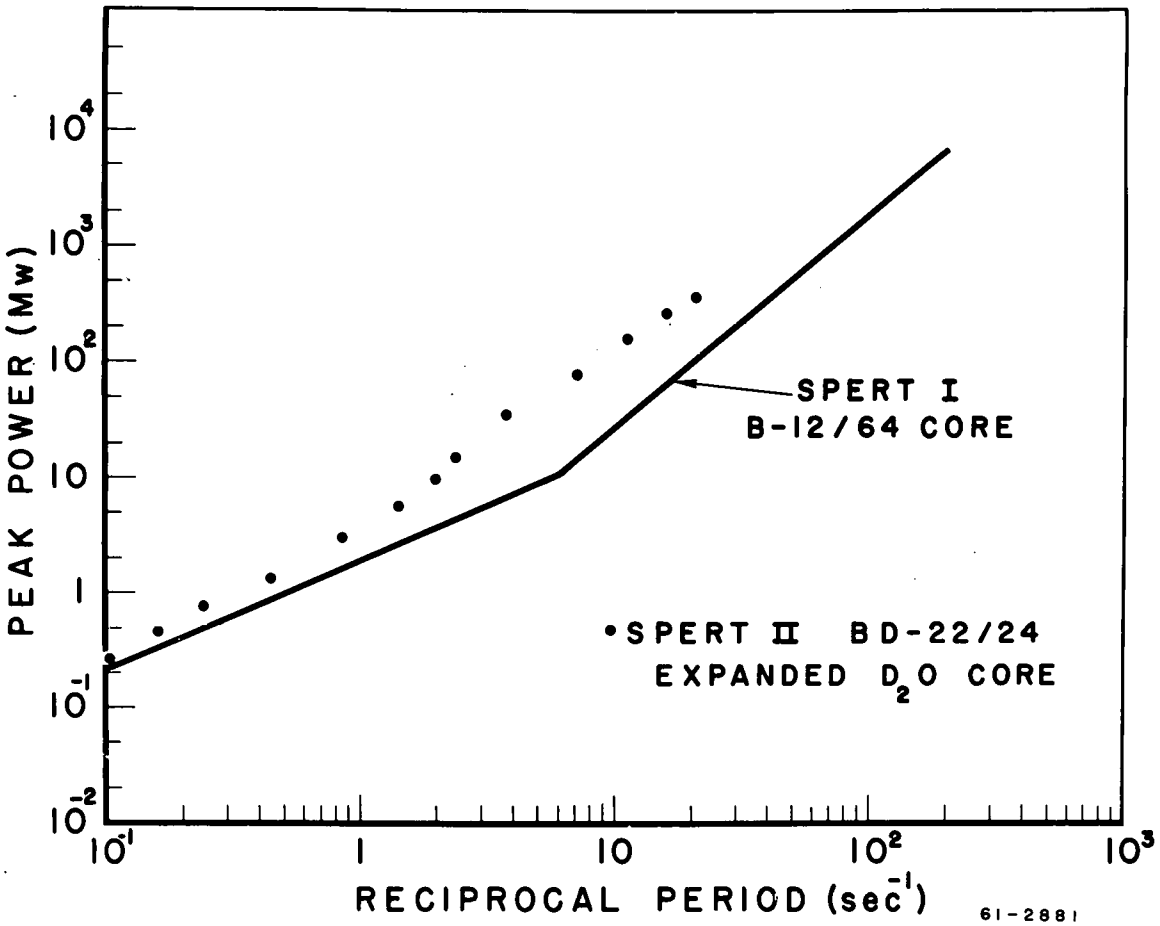

Fig. 5 - Peak Power vs Reciprocal Period for Spert II BD-22/24 Core and Spert I B-12/64 Core

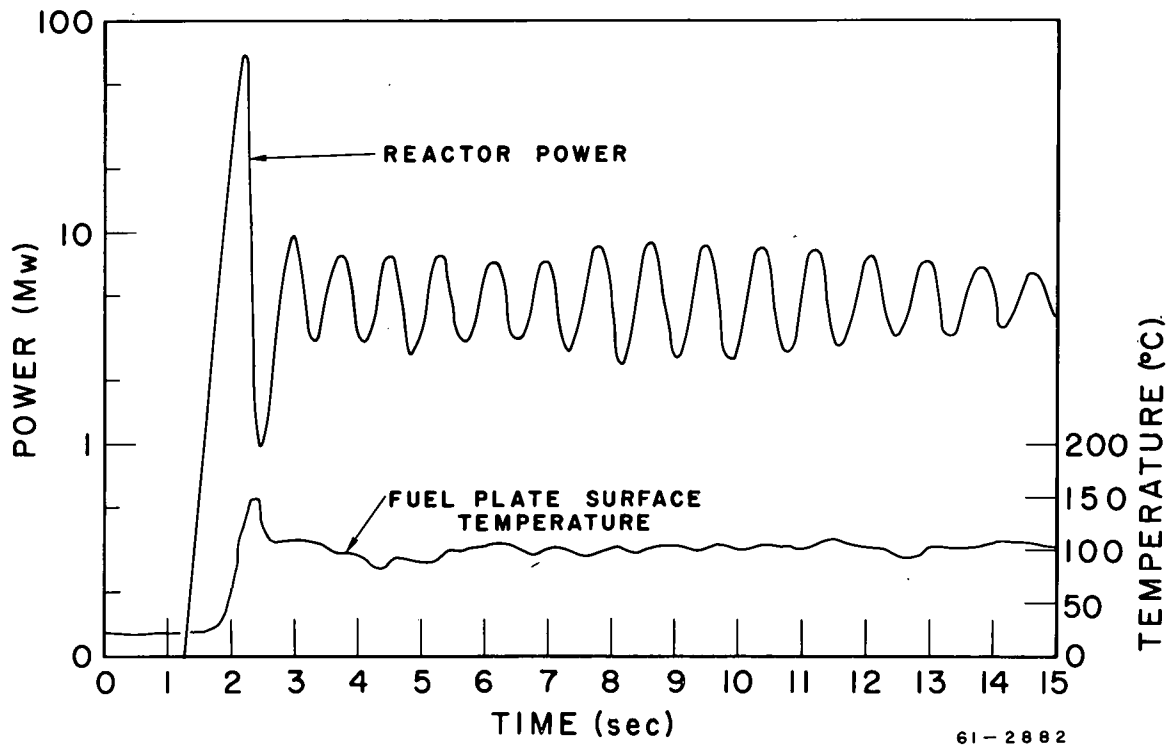

Fig. 6 - Reactor Power and Fuel Plate Surface Temperature for 150 msec-Period Test

to the burst shapes obtained in light-water cores for periods shorter than about 25 msec where boiling had become an important quenching mechanism. The sustained power oscillations following the initial burst were not observed for the light-water power-excursion tests, but are similar to the oscillations observed in the Spert I stability tests when large amounts of reactivity (~ \$1.5) were compensated by steam voids[9]. In short, the power behavior of the D_2O-moderated core for relatively long periods suggests that steam formation is an important mechanism for quenching of the initial burst and that in the post-burst region a substantial amount of reactivity is compensated by boiling. This statement is substantiated by the fuel plate surface temperature data. As shown in Fig. 6, the fuel plate surface reaches saturation temperature prior to peak power and, after an initial overshoot, returns to saturation temperature for the remainder of the test. These results are understandable when the compensated reactivity requirements for the core are considered. For the 150-msec test shown in the figure, approximately \$1.60 is injected to initiate the excursion. Of this, about 70¢ must be compensated at the time of peak power which, for an average void coefficient of $0.02¢/cm^3$ of void,[7] requires that approximately 10% of the moderator within the fuel assemblies must be voided. In the post-burst region almost all of the injected \$1.60 must be compensated, which probably requires bulk boiling. The reactivity compensation due to bulk moderator heating is small in this expanded core configuration, since only the water within the fuel assemblies is appreciably heated.

For a 50 msec-period excursion in this core, about one-third of the D_2O in the assemblies must be voided at the time of the power maximum. This expulsion of D_2O for short-period tests has resulted in differential pressures in the core sufficient to cause bowing of fuel plates. The statistical nature of the bulk boiling process which produces considerable variations in local heat transfer rates has resulted in uncertainty in the location and magnitude of the maximum fuel plate surface temperature.

Detailed examination and correlation of these preliminary data are in progress.

IV. SPERT III

A. Calculations of Nonboiling Reactivity Compensation in Spert III Power Excursions

1. Introduction

In high-pressure systems such as Spert III, it is possible to increase the vessel internal pressure sufficiently to suppress boiling throughout the core up to the time of the peak of a power excursion and thereby eliminate the negative reactivity contribution from steam formation, even in the very short-period region[10,11]. Calculations have been performed in an effort to determine if the predicted reactivity compensation resulting from fuel plate expansion and from conduction heating of the moderator are adequate to account for the observed reactivity compensation at the time of the power peak for nonboiling Spert III power excursions. In this calculation, it is assumed that additional contributions from radiolytic gas formation and direct moderator heating by radiation are relatively small compared with the contributions from the other mechanisms considered, and may be neglected in a first approximation.

A similar approach had been used previously in analyzing some of the Spert I results[12,13] and attained a moderate degree of success. For the Spert III calculations, certain refinements have been incorporated in the calculational technique with the intention of improving the degree of correlation between the calculated values of the reactivity compensated and those obtained from analysis[14] of the reactor power history during the transient.

2. Description of the Analysis

In this analysis, fuel plate expansion and moderator heating are considered to be the reactivity compensating mechanisms. The measured fuel plate surface temperature for the hottest region of the core and the measured neutron flux distribution are used to obtain the local temperature rise in various regions of the core. Thermal expansion of the fuel plates is treated as a decrease in the moderator volume, without net change in the core volume. A one-dimensional thermal diffusion calculation is made to obtain the temperature distribution in the moderator, and the resultant density change, taking proper account of the nonlinear expansion of water, is treated as an effective void volume increase. In order to obtain the reactivity worth of each of these effects, the measured void coefficient of reactivity is suitably adjusted to obtain the local void worth.

Calculations were performed for the Spert III core configuration shown in Fig. 7. The core, which has been described previously[15], consists of 44 plate-type, stainless-steel fuel assemblies and 8 fuel-poison control rods. In the calculations, the relative importance of different regions of the core was taken into consideration by dividing the core into four radial regions, as shown in Fig. 8, and into 18 equal vertical regions. The half-channel water region adjacent to each fuel plate was divided into 33 regions horizontally from the fuel plate surface. The reactivity compensation was then calculated for each local region of the core and the total reactivity compensation obtained by

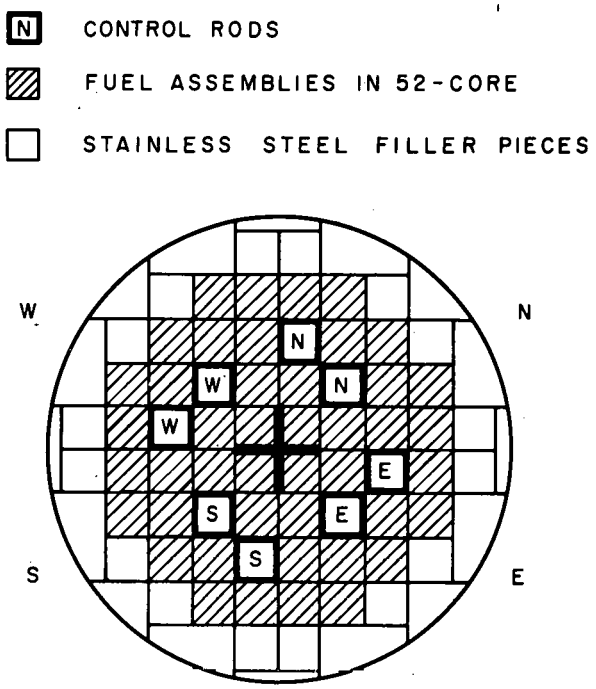

Fig. 7 - Spert III Core Configuration

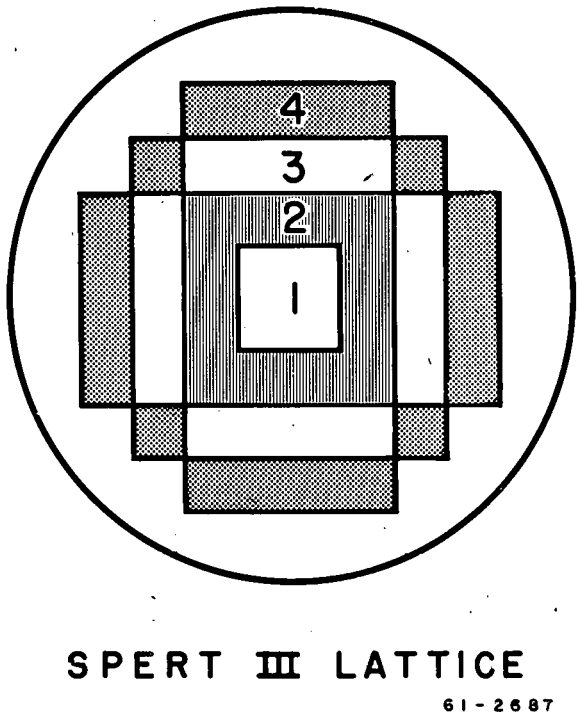

Fig. 8 - Radial Regions for Spert III Reactivity Calculations

summing over all regions of the core.

The reactivity compensated by fuel plate expansion at the time of peak power, Δk_p, was obtained from Eqn.(1).

$$\Delta k_p = \sum_{r,i} C_{r,i} \left(\frac{100}{V_w}\right) \left(3a\, \Delta\theta_{r,i}\right) \left(V_p\right)_{r,i} \qquad (1)$$

where

r = index for radial region = 1, ... 4,

i = index for vertical region = 1, ... 18,

$C_{r,i}$ = the local void coefficient for region (r,i), in ¢/(% of V_w voided),

V_w = total water volume in core,

a = linear expansion coefficient for the fuel plates,

$\Delta\theta_{r,i}$ = average temperature rise in the fuel plates for region (r,i),

and $(V_p)_{r,i}$ = the initial volume of the fuel plates in region (r,i).

The terms of Eqn. (1) were evaluated as follows. In order to determine the local void coefficient $C_{r,i}$, an average void coefficient $\overline{C}_r$ was measured for each radial region, using aluminum strips to simulate voids. $\overline{C}_r$ is expressed in cents per percent of the total core water volume voided. $C_{r,i}$ was assumed to be related to the vertical neutron flux distribution within the radial region r. The vertical variation of void worth and the vertical flux distribution were measured for the central (r = 1) region of the core and it was determined that $C_{r,i}$ is not strictly proportional to the local flux. However, for the calculation it was assumed that the local value of the ratio of the relative vertical void effect to the relative vertical flux $(R.V.E./R.F.)_i$ measured for the central region, is valid for all regions of the core. Then

$$C_{r,i} = \overline{C}_r \left(\frac{\phi_{r,i}}{\phi_r} \right) \left(\frac{R.V.E.}{R.F.} \right)_i \qquad (2)$$

where $\phi_{r,i}/\phi_r$ is the ratio of the average flux for region (r,i) to the average flux for the whole radial region (r).

The average temperature rise of the fuel plate in region (r,i), $\Delta\theta_{r,i}$, was determined by assuming the local surface temperature rise to be proportional to the local neutron flux, $\phi_{r,i}$ and to the measured maximum fuel plate surface temperature rise at the time of peak power, $\Delta\theta_{max}(t_m)$.

Thus,

$$\Delta\theta_{r,i} = b\, \Delta\theta_{max}(t_m) \left(\frac{\phi_{r,i}}{\phi_{max}} \right) \qquad (3)$$

where ϕ_{max} is the maximum measured neutron flux in the core, and b is the ratio of average fuel plate temperature to fuel plate surface temperature, estimated from approximate temperature distribution calculations, and is a function of the reactor period.

Using Equations (2) and (3), Eqn. (1) may then be written more explicitly as

$$\Delta k_p = \sum_{r,i} \overline{C}_r \left(\frac{\phi_{r,i}}{\phi_r} \right) \left(\frac{R.V.E.}{R.F.} \right)_i \left(\frac{100}{V_w} \right) \left(3\, a\, b\, \Delta\theta_{max}(t_m) \left(\frac{\phi_{r,i}}{\phi_{max}} \right) V_p \right)_{r,i} \qquad (4)$$

The second reactivity compensating mechanism considered is moderator heating due to conduction from the fuel plates. Heating of the moderator

from temperature θ_1 to temperature θ_2 results in a fractional density change

$$\frac{\Delta\rho}{\rho} = \frac{\rho(\theta_1) - \rho(\theta_2)}{\rho(\theta_1)} = 1 - \frac{\rho(\theta_2)}{\rho(\theta_1)} \qquad (5)$$

where $\rho(\theta_j)$ = the water density at a temperature θ_j. Since $\Delta\rho/\rho$, thus defined, is equivalent to $\Delta V/V$ for the void coefficient measurements where a volume ΔV of the initial moderator volume is voided, the product of Eqn. (5) and the volume of water in the region (r,i,x), $V(\theta)_{r,i,x}$, is the equivalent void volume associated with that region as a result of heating the moderator from θ_1 to θ_2. It should be noted that Eqn. (5) includes the nonlinear expansion of water with temperature. The total reactivity which is compensated by heat conduction to the moderator is then given by:

$$\Delta k_w = \sum_{r,i,x} C_{r,i} \left(\frac{100}{V_w}\right) \left[1 - \frac{\rho(\theta_2)}{\rho(\theta_1)}\right]_{r,i,x} V(\theta_1)_{r,i,x} \qquad (6)$$

where x = index for water channel regions = 1 ..... 33, $C_{r,i}$ is given by Eqn. (2) and the other symbols are as previously defined. θ_2 was obtained from the average temperature rise of the water in region (r,i,x) based on solution of the one-dimensional thermal diffusion equation for a time-dependent heat input having a burst shape closely approximating that of the experimental power burst. For this solution, the fuel plate surface temperature for a region (r,i), $(\theta_1 + \Delta\theta_{r,i})$, obtained from Eqn. (3), and the fact that the temperature remains finite were used as the boundary conditions.

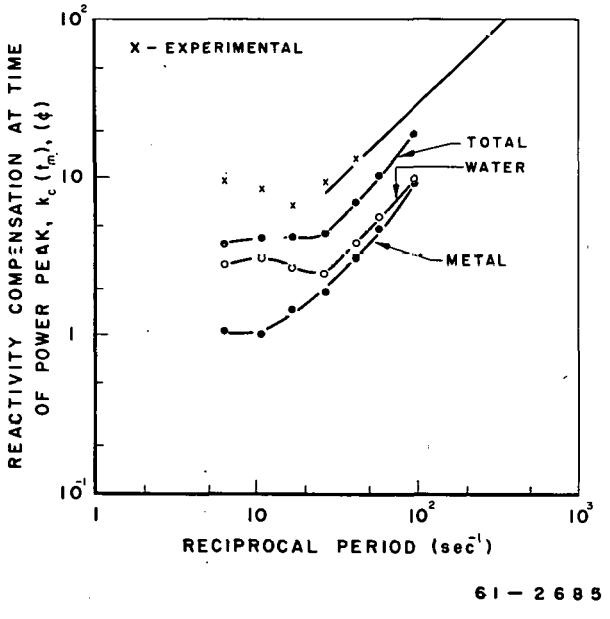

Fig. 9 - Comparison of Experimental and Calculated Values of Reactivity Compensated at the Time of Power Peak

The total reactivity compensated to the time of peak power is given by the sum of the individual contributions from moderator heating, Eqn. (6), and fuel plate expansion, Eqn. (4).

3. Comparison of Calculations with Experimental Results

In Fig. 9, the results of the calculations are presented together with the experimental values of the reactivity compensated to the time of the power peak for seven step-transient power excursions at elevated pressures in the Spert III reactor. These tests ranged in values of the reciprocal

period from 6 to 95 reciprocal seconds, corresponding to initial periods of 167 msec to 10.5 msec. The curve marked "total" is the sum of the lower curve, Δk_p, and the next higher curve, Δk_w. The experimental values of the total reactivity compensated to the time of the power peak, as determined from analysis of the power history, are shown as data points. A value of ℓ/β_{eff} of 3×10^{-3} sec, where ℓ is the prompt neutron lifetime and β_{eff} is the effective delayed neutron fraction, was used. As can be seen from the figure, the present calculational approach produces the general shape of the compensated reactivity dependence on reciprocal period for reciprocal periods greater than 20 sec^{-1}, but yields values which are only about half as large as the experimental values.

Since it is recognized that errors exist in the input data, the sensitivity of the analytical results was investigated for variations in each of the input parameters. By considering a maximum possible deviation of 20% in all of the quantities involved in the calculations, a probable deviation of 50% has been determined for the calculated values of the reactivity compensated to the time of the power peak. Even with this liberal allowance for errors in the input parameters, the experimental values are still outside the limits estimated for the calculated values.

As a further check on the validity of the calculational method, this technique with all its refinements was applied to some long-period, nonboiling, Spert I test data and yielded discrepancies with the experimental data similar to those resulting from the Spert III calculations.

The results of these calculations indicate that the method of analysis used does not account for the observed reactivity compensation at the time of the power maximum for nonboiling power excursions if fuel plate expansion and moderator heating by conduction are the only reactivity compensating mechanisms considered. Although the previous,[13] less detailed, calculations and experimental results indicated that radiolytic gas formation and moderator heating by neutron and gamma radiation were not important for short-period tests, a reconsideration of the magnitude of such effects is in order. The possibility also exists that previously unexplored radiation effects on heat transfer rates may have become manifest, which could result in greater reactivity compensation from water expansion.

B. Ramp-Initiated Power-Excursion Tests

Tests have been performed to investigate the response of the Spert III reactor to reactivity additions which are linear functions of time. These ramp insertions of reactivity were initiated from delayed critical at room temperature (~ 25°C) for various initial power levels from 0.1 w to 100 kw, system pressures from 0 to 2500 psig, and coolant flow rates from 0 to 20,000 gpm. Reactivity addition rates of 53¢/sec, 35¢/sec and 18¢/sec were used. All tests were terminated shortly after the occurrence of the initial power burst.

The effect of ramp rate on the initial power burst is shown in Fig. 10. The reactor power is shown as a function of time after the start of the reactivity addition for tests having ramp rates of 53, 35 and 18¢/sec. Each of the tests was initiated from a power level of about 10 w, with a system at atmospheric pressure and with no forced coolant flow. The factor of three increase in ramp rate resulted in a factor of five increase in peak power, from about 90 Mw to about 450 Mw. The minimum effective periods were 17, 23 and 42 msec for the ramp rates of 53, 35 and 18¢/sec, respectively.

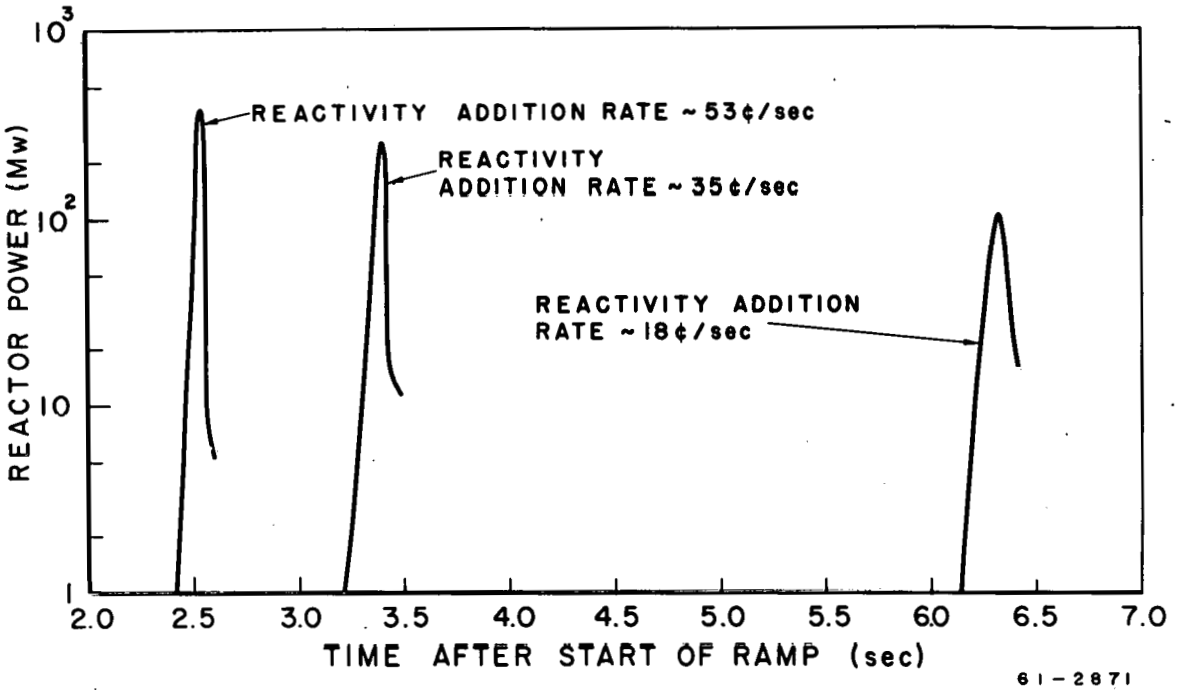

Fig. 10 - Reactor Power Behavior for Room Temperature, Atmospheric Pressure, No-Flow Excursions with Ramp Rates of 53, 35 and 18¢/sec (Initial Power = 10 w)

The effect of initial power level on the power burst shape is shown in Fig. 11 for 18¢/sec ramp-rate tests performed at atmospheric pressure with no flow. The factor of 10^6 decrease in initial power from 100 kw to 0.1 w resulted in a factor of about twenty increase in peak power. The reactivity addition is also shown as a function of time and it is noted that, in all cases, the power maximum occurred prior to the end of the reactivity addition. The observed relative insensitivity of the peak power to initial power is in essential agreement with previous Spert I data(16) and with predictions of an analytical model previously reported(16,17,18).

The approximate analytical model for ramp-burst behavior indicates that for super-prompt-critical excursions, the power behavior for ramp-induced and step-induced bursts will be quite similar when the two are compared on the basis of effective period; that is, when the minimum effective period for the ramp burst equals the initial asymptotic period for the step burst. In Fig. 12, the reactor power behavior is shown for an 18¢/sec ramp test and a 40 msec-period step test. The minimum period

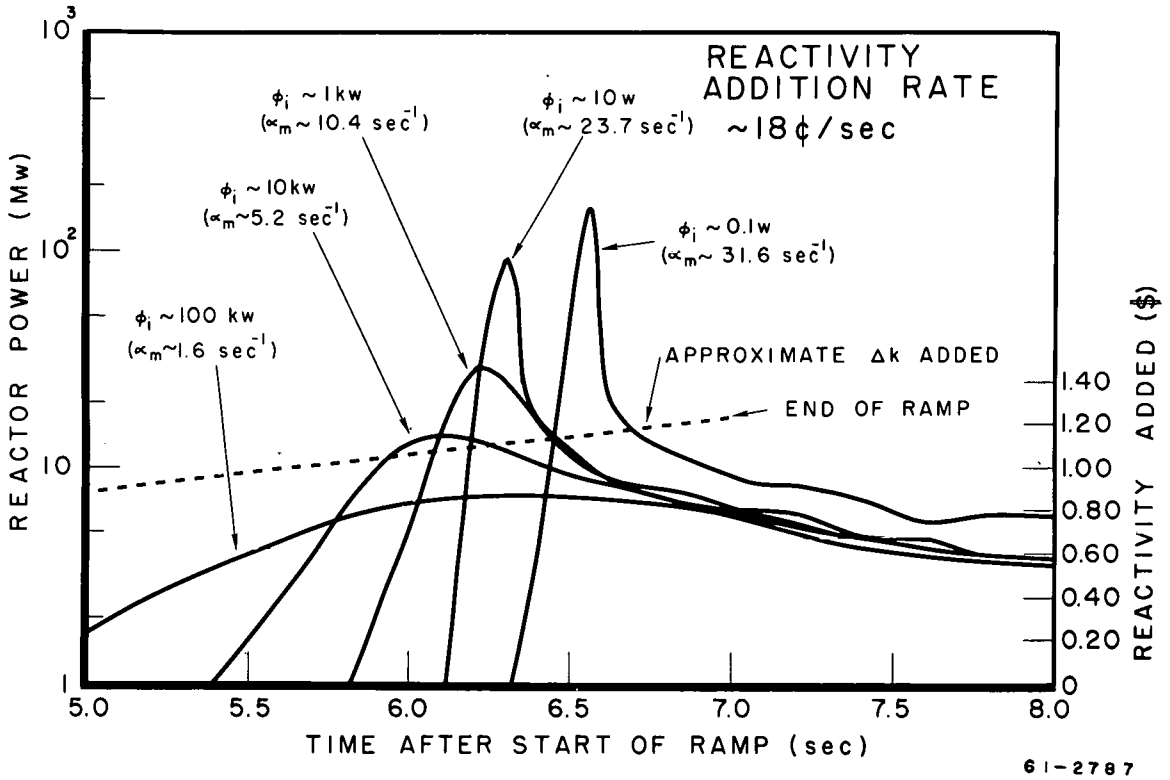

Fig. 11 - Reactor Power Behavior for Room Temperature, Atmospheric Pressure, No-Flow Excursions with Initial Power as a Parameter (Ramp Rate = 18¢/sec)

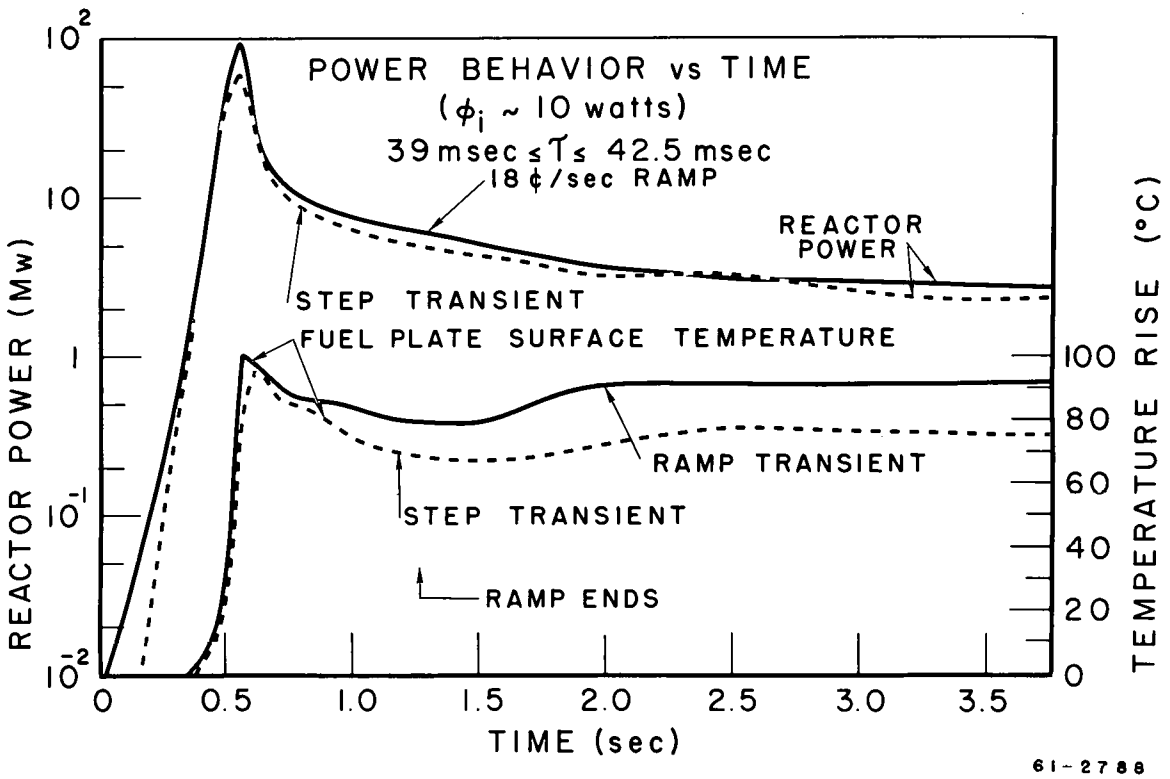

Fig. 12 - Reactor Power and Fuel Plate Surface Temperature for 18¢/sec Ramp Test and 40 msec-Period Step Test

for the ramp test is about 42 msec. Both excursions were initiated from a power of 10 w with atmospheric pressure and zero flow. The peak power for the ramp test is slightly higher, but otherwise the bursts are quite similar. The fuel plate surface temperatures for the hottest measured fuel plates are also compared in Fig. 12 and are seen to be essentially the same.

Fig. 13 is a similar comparison of a 53¢/sec ramp-rate test (τ_{min} ~ 17 msec) with a 17.5 msec-period step excursion. The peak powers agree within a factor of two but there is a noticeable difference in the undershoot immediately following the burst. Since the reactivity which must be compensated at the time of the power peak is larger for the ramp, as evidenced by the higher power maximum, the delay in energy transport from fuel plate to water results in a larger overcompensation in reactivity after the peak, producing the greater undershoot. If this same ramp burst is compared with a 14 msec-period step test, both the power peak and the post-burst behavior agree very closely.

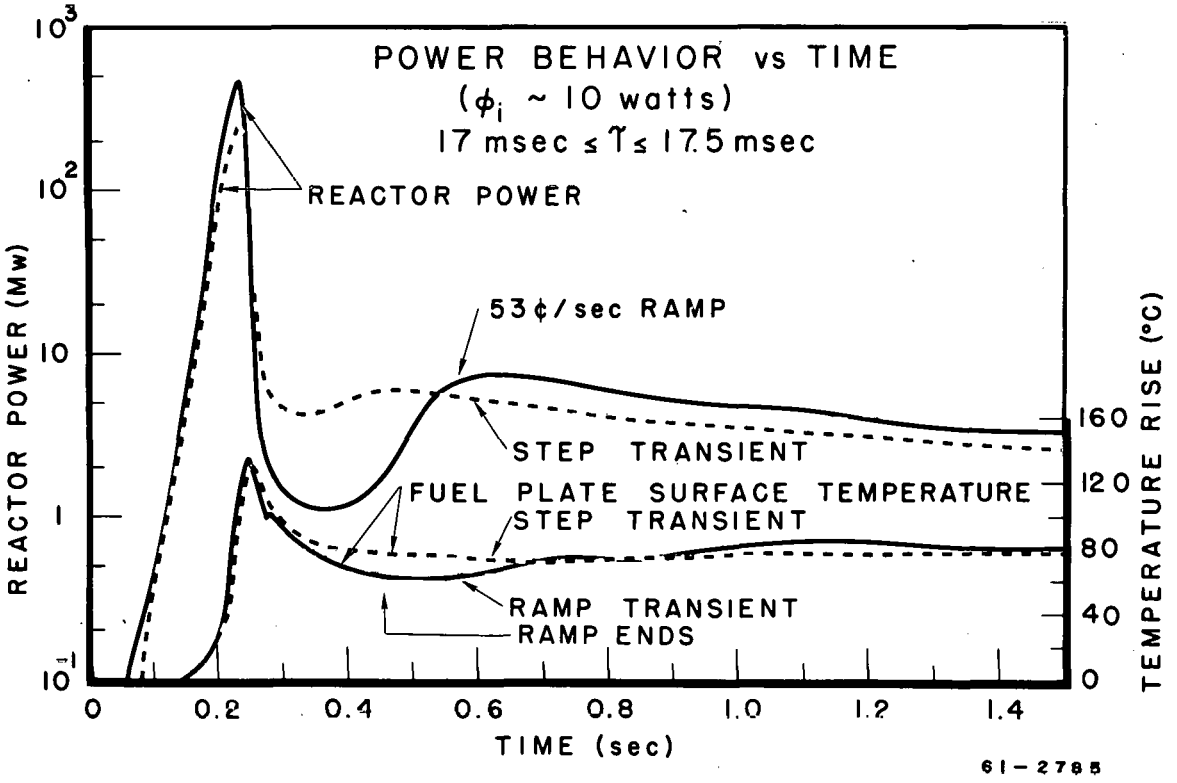

Fig. 13 - Reactor Power and Fuel Plate Surface Temperature for 53¢/sec Ramp Test and 17 msec-Period Step Test

Fig. 14 is a plot of the maximum reactor power as a function of maximum reciprocal period for all of the atmospheric pressure, no-flow ramp tests, at all addition rates and initial power levels. The dashed line is the best-fit line for step-insertion test data in Spert III. It is seen that the equivalence on the basis of period is good within about a factor of two between step- and ramp-insertion tests, even for long-period tests for which the "prompt approximation" analytical model does not strictly apply. Similar results had been found previously for Spert I tests[16].

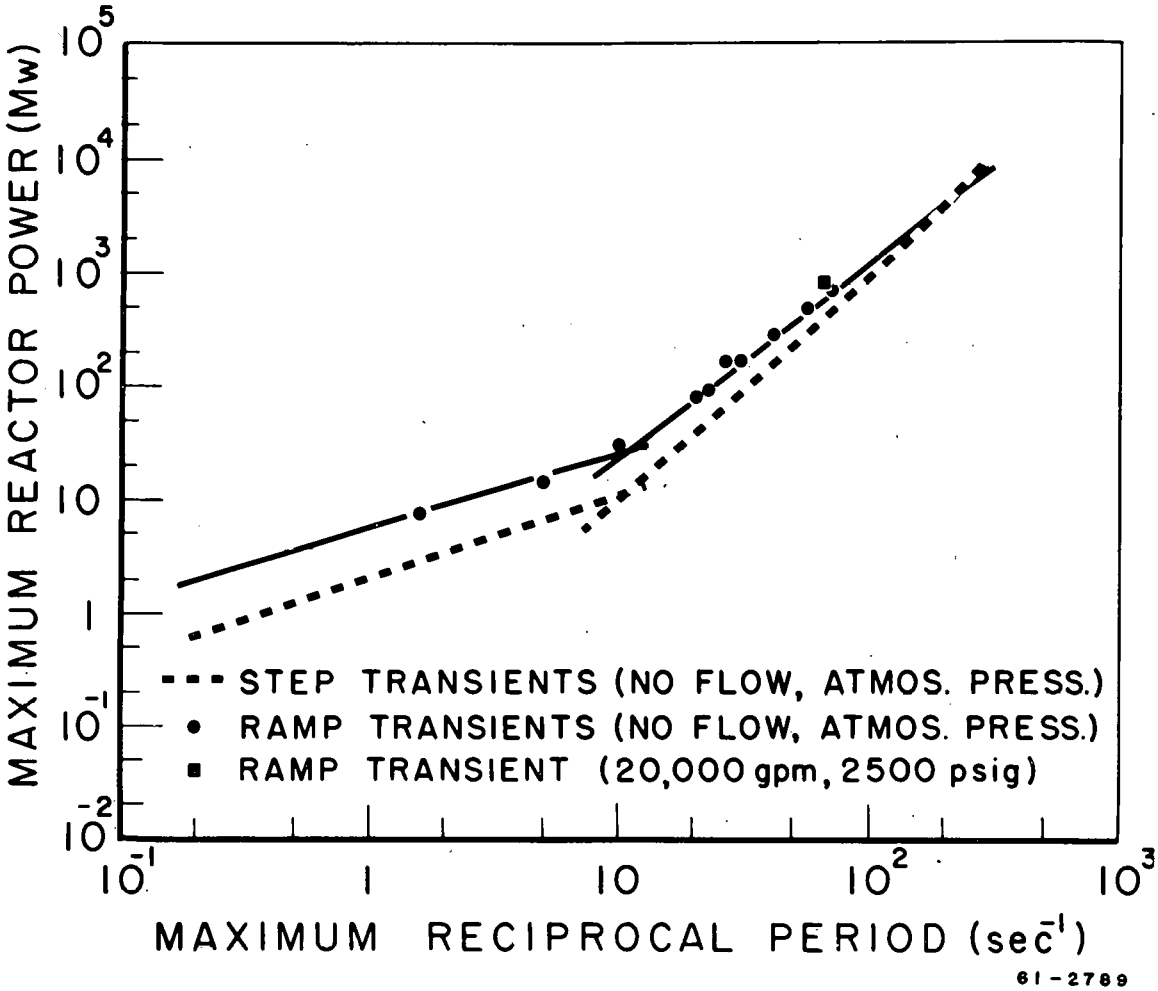

Fig. 14 - Maximum Reactor Power vs Maximum Reciprocal Period for Spert III Ramp Tests

The effects of changes in system pressure and coolant flow rate on the kinetic behavior for ramp insertions were found to be essentially the same as those found for step insertions[19]. A single data point for a ramp test at 20,000 gpm flow and a pressure of 2500 psig has been included in Fig. 14 to indicate the relative insensitivity of peak power to changes in these parameters.

In summary, the Spert III ramp-induced power-excursion tests at room temperature have shown that, as was the case for the Spert I reactor, power burst behavior is quite sensitive to reactivity addition rate, and relatively insensitive to initial power level in the range from 0.1 w to 100 kw; and that, for practical purposes, ramp- and step-induced bursts are essentially equivalent when compared on the basis of effective period. In addition, it has been demonstrated that the effects of changes in system pressure and flow rate on power excursion behavior are essentially independent of the mode of reactivity insertion.

V. ENGINEERING

A. Spert III Thermowell Failure

During a recent mechanical disassembly of the Spert III core structure, the immersion section of a primary system thermowell was found in the bottom of the Spert III reactor vessel. Investigation showed the broken thermowell to be a spare which had been plugged during plant construction. Had this not been the case, the failure would have been immediately indicated by a leak in the primary coolant system. The broken thermowell had originally been located in the east loop of the primary piping between the discharge of the primary coolant pumps and the inlet to the reactor vessel. Circulation of the coolant had apparently carried the broken section of the well from its original position into the reactor vessel where it was found.

Examination of the broken thermowell revealed it to have been "field-fabricated" from an 8-in. length of 1/2-in., schedule 80, stainless-steel pipe, the inner end of which was seal-welded. The other end was welded into a 1-in. by 1/2-in., stainless-steel bushing. The thermowell assembly had been installed in the primary system by threading the bushing into a 1-in. stainless-steel pipe boss which is welded to the primary piping. The threaded joint had been seal-welded. The break occurred at the weld of the 1/2-in. pipe to the bushing. A metallurgical examination of the break indicated a typical fatigue failure with no evidence of intergranular corrosion.

A subsequent check of the 18 thermowells in the Spert III primary piping system revealed that 12 were commercially supplied wells with a 9-in. immersion length, two were commercially supplied wells with a 6-in. immersion length, and the remaining five were "field-fabricated" with approximately an 8-in. immersion length. All of the thermowells were of the cantilever-type and were installed perpendicular to the flow stream.

The five "field-fabricated" thermowells were immediately removed from the system since details of their construction were not available. An analysis was initiated to evaluate the suitability of the remaining wells for this service. Calculations were made to determine pertinent characteristics[20] of the remaining wells and of a commercial 5-in. immersion-length well being considered for replacement of the "field-fabricated" wells. The results of these calculations are shown in Table 2.

Since the calculated natural frequency in air of the 9-in. well fell between the Karman vortex frequency (due to flow velocity) and the primary coolant pump impeller frequency (~ 350 cps), additional evaluation of this well was required. The calculational method used to obtain the natural frequency of the thermowells in air generally gives an answer lower than the actual experimentally obtained frequency[20]. In addition, a water medium is known to lower the natural frequency of an immersed body[21]. A laboratory experiment was conducted on an available 5-in. immersion-length well to test an experimental method for obtaining the frequency response of the installed plant thermowells and to estimate the water immersion effect on the natural frequency.

TABLE 2

CALCULATED THERMOWELL CHARACTERISTICS
(Based on 30 ft/sec (70°F) Water Flow Velocity)

	Type of Well (Immersion Length)		
	9-in.	6-in.	5-in.
Static Pressure Limitation, 700°F (psi)	4050	4050	4280
Natural Frequency in Air, 70°F (cps)	300	675	890-965*
Immersion Length Limit (in.)	17	17	17
Karman Vortex Frequency (cps)	106	106	115

*Calculational constants were approximated for this well[20].

Strain gages were installed on the inside and the outside of the thermowell and the well was threaded into a heavy steel plate. The outputs of the strain gages were amplified and fed into an oscilloscope. Rapping the thermowell produced a strain gage signal which was observed on the oscilloscope and photographed. The natural vibration frequency of the thermowell was estimated from the photograph. Several photos were taken with the well both in air and immersed in water. From this experiment, it was found that the natural frequency in air was 1020 cps and the natural frequency in water was 950 cps for the 5-in. well.

Experimental data were also obtained for the Spert III plant thermowells in place. The frequency characteristics were determined for various coolant flow rates. For these tests, strain gages were mounted inside a 9-in. immersion-length well, a 6-in. well and a 5-in. well. The 5-in. thermowell was a replacement for one of the "field-fabricated" wells that had been removed from the system. Outputs of the strain gages were amplified, observed on an oscilloscope and recorded on magnetic tape. The natural frequency of each thermowell type was obtained by rapping the top of the well and photographing the signal output on the oscilloscope. The frequencies observed with the primary system filled with water were:

9-in. immersion-length well - ~350 cps
6-in. immersion-length well - ~730 cps
5-in. immersion-length well - ~970 cps

Plant flow conditions of 6,000 gpm, 12,000 gpm and 20,000 gpm were established for testing the 5-in. and 9-in. immersion-length thermowells, and flows of 500 gpm, 1000 gpm and 1500 gpm were established for testing the 6-in. immersion-length thermowell. The strain gage output signals were recorded on magnetic tape. Figures 15, 16 and 17 show the results of a 1/2 octave band frequency analysis of the strain gage output signals.

It is apparent from the figures that the amplitude of excursion of the 9-in. thermowell in the region of its natural frequency, 350 cps, is as much as 80 times that of the excursions for frequencies other than 350 cps. Flow rate has little effect on this amplitude which indicates that vortex excitation is relatively unimportant. However, since the natural frequency of this thermowell coincides very closely with the primary pump impeller frequency, the amplitude gain is undoubtedly due to excitation of the thermowell by pump operation.

The 6-in. thermowell is somewhat excited near its natural frequency, 730 cps; however, the maximum amplitude of the excursions in this region is only a factor of 20 times that of the excursions in other frequency regions. Since this excitation occurs at about one octave above the impeller base frequency, it can also probably be attributed to the pump impeller frequency.

The 5-in. well is relatively unaffected by either flow or pump frequencies.

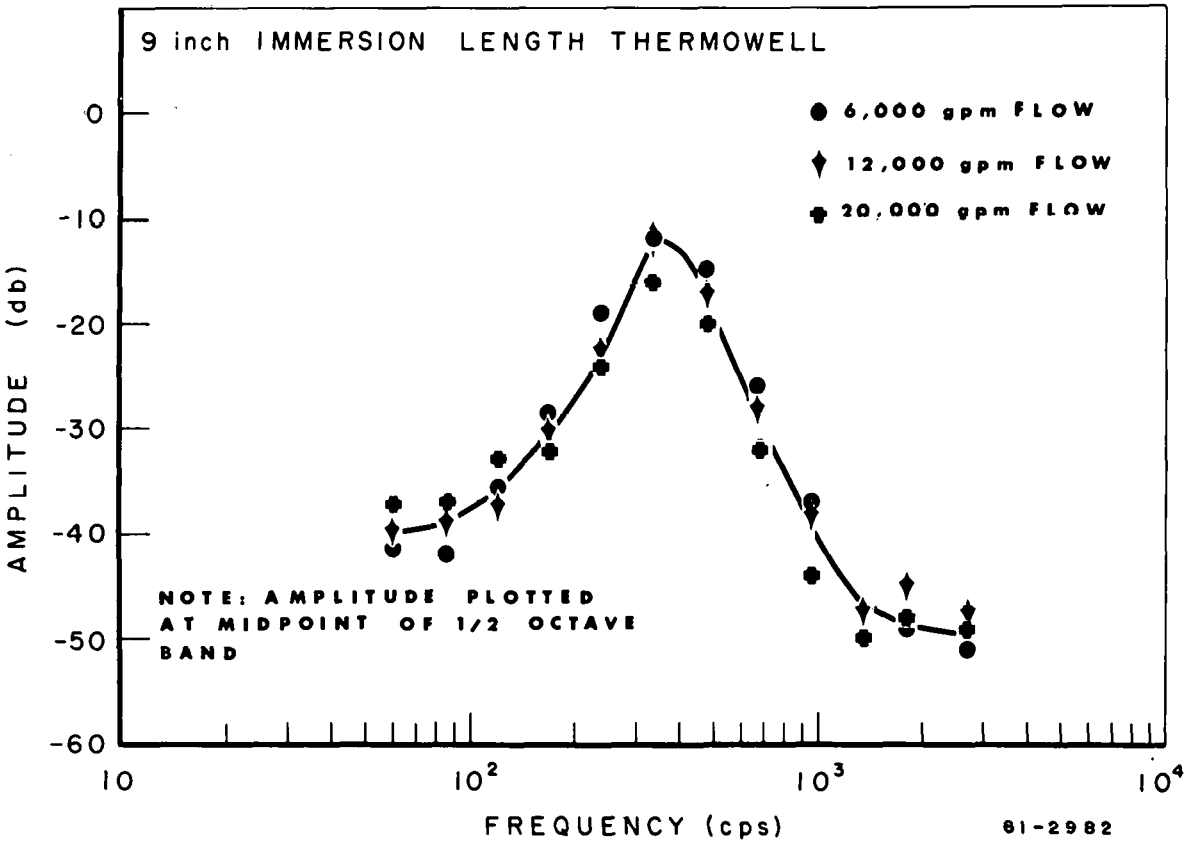

Fig. 15 - Vibration Frequency Spectrum for 9-in. Immersion-Length Thermowell

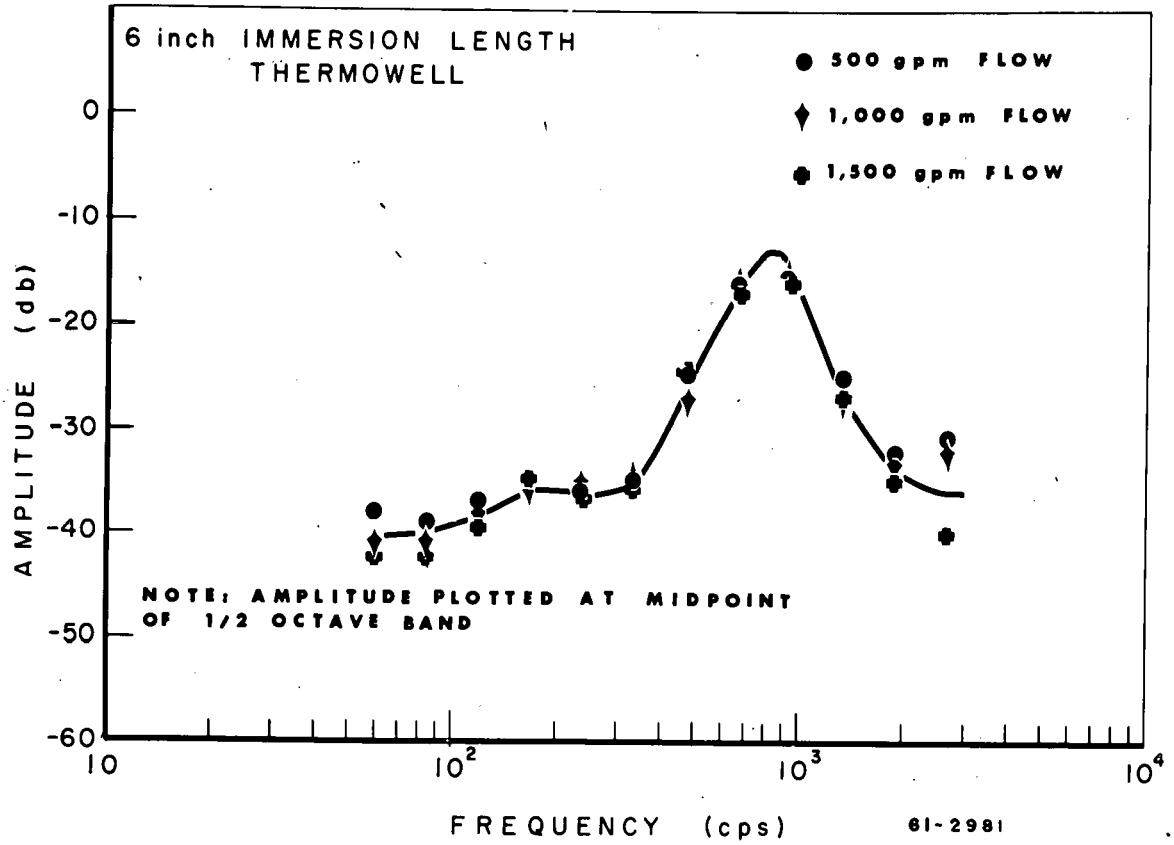

Fig. 16 - Vibration Frequency Spectrum for 6-in. Immersion-Length Thermowell

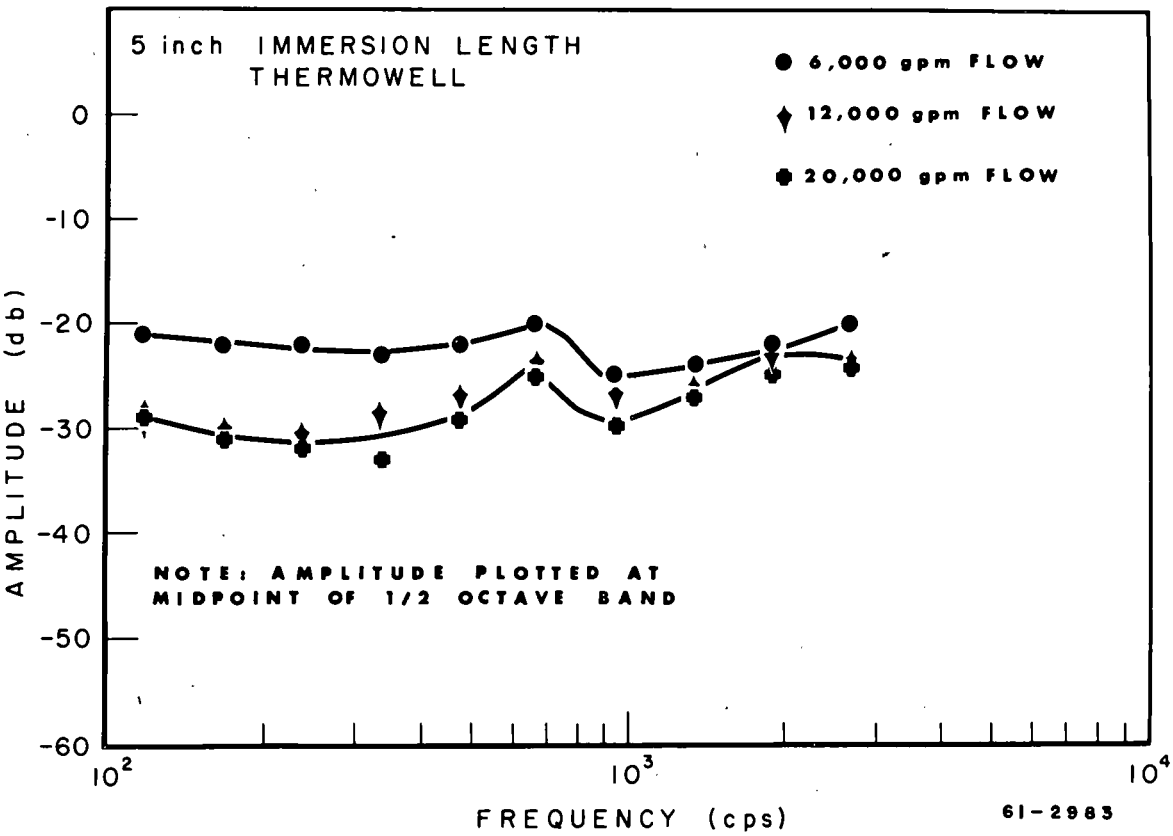

Fig. 17 - Vibration Frequency Spectrum for 5-in. Immersion-Length Thermowell

It thus appears that the use of the 9-in. and 6-in. thermowells in the Spert III system had not been adequately evaluated in the original plant design. In view of the possible consequences of future fatigue failures during plant operation, which could include serious damage to the canned-rotor pump impellers, and in consideration of the above data, all of the 9-in. immersion-length thermowells which are subjected to high velocity flow were removed from the primary system and replaced with 5-in. immersion-length thermowells.

B. Spert Type "D" Assembly Hydraulic Fatigue Test

A hydraulic fatigue test has been conducted on the 18-plate, type "D" fuel assembly[22] intended for use in Spert IV. The assembly was subjected to a flow of 590 gpm for 220 hours in the MTR-ETR hydraulic test facility. This flow represented an average velocity of 41 ft/sec in the fuel assembly water channels and a fuel assembly pressure drop of 43 psi. This flow rate is approximately 300% of the maximum flow rate proposed for use in Spert IV.

At the completion of the test, the fuel assembly was dismantled and the U^{238} dummy fuel plates were inspected. No apparent physical damage occurred to the plates except for a slight longitudinal bowing which could only be observed after the plates were removed from the assembly.

VI. REFERENCES

1. R. M. Ball, et al., "Critical Experiments for the NS Savannah Core", BAW-1131 (December 10, 1958).

2. "Quarterly Technical Report, Spert Project", July, August, September, 1960, F. Schroeder, ed., IDO-16677, pp. 6-7 (1961).

3. Z. Akcasu, "General Solutions of the Reactor Kinetic Equations Without Feedback", Nuclear Sci. and Eng., 3, pp. 456-7 (April 1958).

4. F. Kirn, et al., "Reactor Physics Measurements in Treat", ANL-6173 (October 1960).

5. G. R. Keepin and T. F. Wimett, "Reactor Kinetics Functions; A New Evaluation", Nucleonics 16, (10), pp. 86-90 (October 1958). G. R. Keepin, T. F. Wimett and R. K. Zeigler, "Delayed Neutrons from Fissionable Isotopes of Uranium, Plutonium and Thorium", Phys. Rev., 107, p. 144 (1957).

6. Reference 2, pp. 9-11.

7. "Quarterly Technical Report, Spert Project", October, November, December, 1960, F. Schroeder, ed., IDO-16687, pp. 5-8 (1961).

8. S. G. Forbes, et al., "Analysis of Self-Shutdown Behavior in the Spert I Reactor", IDO-16528 (July 23, 1959).

9. F. Schroeder, "Stability Tests with the Spert I Reactor", IDO-16383 (July 1, 1957).

10. "Quarterly Technical Report, Spert Project", April, May, June, 1960, F. Schroeder, ed., IDO-16640, pp. 20-24 (April 7, 1961).

11. Reference 7, pp. 9-14.

12. S. G. Forbes, "Quarterly Progress Report, Reactor Projects Branch", July, August, September, 1958, G. O. Bright, ed., IDO-16512, pp. 28-48 (May 6, 1959).

13. Reference 8, pp. 33-39.

14. R. W. Miller, "Calculations of Reactivity Behavior During Spert I Transients", IDO-16317 (June 1, 1957).

15. F. Schroeder, W. J. Neal, C. R. Toole and R. A. Zahn, "The Spert III Reactor Nuclear Startup", IDO-16586 (March 18, 1960).

16. Reference 8, pp. 25-32.

17. W. E. Nyer, "Quarterly Progress Report, Reactor Projects Branch", January, February, March, 1958, G. O. Bright, ed., IDO-16452, pp. 65-70 (August 5, 1958).

18. S. G. Forbes, "The Dependence of Reactor Behavior on the Self-Shutdown Mode", IDO-16635, pp. 19-35 (April 25, 1961).

19. Reference 7, pp. 9-16.

20. J. W. Murdock, "Power Test Code Thermometer Wells", Trans. ASME, Journal of Engineering for Power, 81, Series A, No. 4, pp. 403-416 (October 1959).

21. P. M. Morse, "Vibration and Sound", pp. 104-105, 2nd ed., McGraw-Hill (1948).

22. "Quarterly Technical Report, Spert Project", January, February, March, 1960, T. R. Wilson, ed., IDO-16617, p. 19 (March 31, 1961).

PHILLIPS
PETROLEUM
COMPANY

ATOMIC ENERGY DIVISION